# Surface modification of LiFePO4 nanoparticles through an organic/ inorganic hybrid approach and its impact on electrochemical properties

Ana Cristina Martinez, Walid Dachraoui, Rajesh Murugesan, Emmanuel Baudrin, Arnaud Demortiere, Matthieu Becuwe

Version of Record: https://www.sciencedirect.com/science/article/pii/S0927775722007075
Manuscript_efb1b84391900b751bc3797d1715508b

# Surface modification of $LiFePO_4$ nanoparticles through an organic/inorganic hybrid approach and its impact on electrochemical properties

Ana Cristina Martinez,[a-c] Walid Dachraoui, [a-c] Rajesh Murugesan,[a-c] Emmanuel Baudrin,[a-d] Arnaud Demortière, [a-d] Matthieu Becuwe* [a-d]

[a] Laboratoire de Réactivité et Chimie des Solides (LRCS), UMR CNRS 7374, Université de Picardie Jules Verne, 33 rue Saint-Leu, 80039 Amiens Cedex, France.

[b] Institut de Chimie de Picardie (ICP), FR CNRS 3085, Amiens Cedex, France.

[c] Réseau sur le Stockage Electrochimique de l'Energie (RS2E), FR CNRS 3459, France.

[d] ALISTORE-European Research Institute, FR CNRS 3104, Hub de l'Energie, Rue Baudelocque, 80039 Amiens Cedex, France.

## Abstract

For the first time, chemical surface modification, using an hybrid organic/inorganic approach and its impact on the electrochemical response of a nanometric lithium iron phosphate obtained by the facile solvothermal method using an organic capping agent is investigated. Removal of the capping agent was realized through different approaches, such as washing with an organic solvent, chemical treatments, and ligand exchange with redox mediator having electrochemical activity close or not to the one of the material, to maintain the material's morphology and structure. The redox mediator grafting approach appears very interesting, since an unpredicted impact on the electrochemical activity of the material was observed. In that case, while materials structure and morphology are fully preserved, a more or less important change of the electrochemical curve shape depending on the redox potential of the grafted molecule was observed, which suggest that this approach could be a good

alternative to traditional carbon coating, facilitate recycling and bring new functionalities to positive electrode materials.

**Keywords:** Organic/Inorganic Hybrid material, surface chemistry, nanomaterials, energy storage, lithium-ion batteries.

## 1. Introduction

The energetic context prompts the search for efficient and low-cost energy storage technologies either as an energy reservoir for supplying electronics, engines or as a buffer for grid applications to stabilize intermittent renewable energy production. Ion-based electrochemical storage systems (*i.e.* Li-ion and Na-ion batteries) stand as some of the best solutions to address such challenges,[1] inducing many efforts to improve batteries performances in terms of energy density and power density.[2] One of the most noteworthy achievement concerns the drastic reduction of particle size towards the nanometer scale, which led to an improvement of the rate capability of the related electrodes thanks to the reduction of ion/electron motion path in the solid.[3–6] Despite this achievement, and particularly for electronic powering or for hybrid and electric vehicles, nanomaterial-based electrodes were exploited with a lot of difficulties mainly due to the intrinsic properties of nanoparticle (high surface reactivity, parasite reactions, larger SEI and rheology).[7]

Even if the decrease of motion length helps to improve the kinetics, the electronic conductivity of the composite electrode is determining for efficient storage systems. In the case of positive electrode materials, ideally, the active material is coated with a carbon-based conductive layer formed by pyrolysis of organic compounds under specific conditions.[8–10] Such an energy-consuming process is difficult to be applied to thermal-sensitive materials, such as fluorosulphates,[11] as well as nanomaterials for which high temperature induces nanoparticles coalescence which is finally affecting the cycling kinetics. One promising and more sustainable alternative to enhance the performance of positive electrode materials

without a high-temperature annealing is to take advantage of the versatility of organic compounds through an organic/inorganic hybrid approach to realize an on-demand functional engineering.[12]

Defined over the ’90s, hybridization of inorganic compounds using organic substances is a powerful tool to create an “unlimited” range of materials having specific, innovative and synergistic properties for multiple application fields.[13] One of the best examples of synergistic hybrid material in the energy field is of course the development of Dye-Sensitized Solar Cells (DSSC) that combine energy levels of an metal-organic compound and titanium oxide nanoparticles to harvest sunlight and produce electrical energy.[14,15] On the electrochemical energy storage side, the organic-inorganic hybrid approach appeared a few years later with studies involving conducting polymers associated with Polyoxometallates (POMs) and carbon-based organic compounds.[16–19] Based on work realized on the DSSCs, a striking example of hybridization was the sensibilization of the electroactive compounds (i.e. $LiFePO_4$), leading to the first example of carbon-free thin electrodes and redox-targeting of the insertion materials with redox mediators.[20–22] More recently, rate performances and electrochemical cycling kinetics have been improved by hybridization of the electrode through the clever incorporation (without strong interaction or grafting) of an ultra-fast and non-conjugated redox polymer during the formulation process. For example with $LiFePO_4$ (LFP),[23,24] this mediation concept was judiciously extended to high-voltage materials like $LiMn_2O_4$ (LMO)[25] and $LiCoO_2$ (LCO)[26] to boost kinetics and decreasing the overpotential.

Convinced that the organic/inorganic hybrid approach will be at the centre of the interface managing for the fabrication of smart and functional electrodes (including self-healing phenomenon, sensing properties and interface managing), we propose here to combine redox targeting and surface grafting. With this aim, a preliminary study focused on the chemical surface modification of nanometric LFP is proposed for the first time. To

observe the impact of the surface modification on the electrochemical response, we selected as model material a capped nanometric LFP (OlAm-LFP) obtained by a solvothermal synthesis using Oleyl amine (OlAm) as a reducing and capping agent.[27] Firstly, OlAm-LFP was washed using either organic solvents mixture or weak carboxylic acid to remove oleylamine and clean/deliver the surface (Figure 1). Alternatively, ligand exchange reactions were carried out using two organic redox active molecules possessing a carboxylic acid function (4-carboxy-TEMPO and 2-carboxy-Anthraquinone) to study how the electrochemical activity of the redox mediators impact on the electrochemical response of the inorganic positive electrode material.

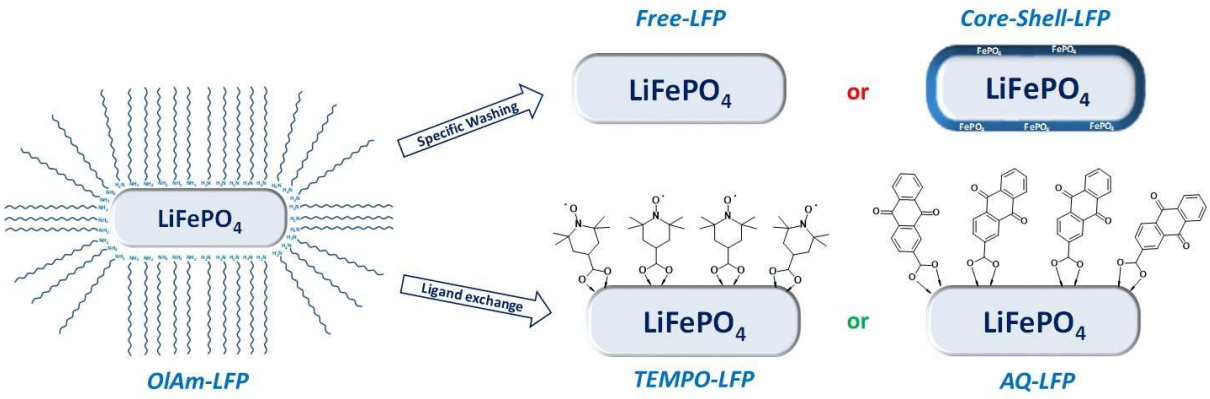


**Figure 1: Scheme of the different routes to remove the capping agent on OlAm-LFP either by specific washing using organic solvent (Free-LFP) and weak acid (Core-shell-LFP) or by ligand exchange using 4-carboxy-TEMPO (TEMPO-LFP) and 2-carboxy-anthraquinone (AQ-LFP).**

## 2. Experimental

### 2.1 Reagents and chemical

Lithium iodide (LiI), diammonium phosphate ($(NH_4)_2HPO_4$), iron(II) chloride ($FeCl_2$), oleylamine ($C_{18}H_{35}NH_2$, OlAm) and 1-octadecene ($C_{18}H_{36}$) were obtained from Sigma-Aldrich and used without further purification. 4-carboxy-TEMPO and 2-carboxy-Anthraquinone were obtained from Acros Chemicals and used as received.

### 2.2 Characterization tools

X-ray diffraction (XRD) patterns were obtained using a Brücker X-ray diffractometer equipped with Cu Kα radiation. The accelerating voltage and current were 40 kV and 100 mA, respectively. The XRD patterns were collected in the 2θ range of 15–55° using a continuous scan mode with a step size of 0.02° and a scan rate of $4°.min^{-1}$. FTIR spectra in diffuse reflectance mode were obtained by acquiring 150 scans at room temperature over a range of 4000-400 $cm^{-1}$, by means of a Nicolet AVATAR 370 DTGS spectrometer from Thermo Electron Corporation. TEM analyses (HRTEM), such as TEM imaging and selected area electron diffraction (SAED), were carried out using a FEI Tecnai G2 F20 S-TWIN (S)TEM. The SAED pattern simulation and image processing was performed using MacTempasX2 (based on $LiFePO_4$ (Pnma) CIF file) and FIJI softwares, respectively. The electrochemical properties of nanostructured materials were studied by assembling two-electrode Swagelok-type cells inside an Ar-filled glove box. The cathode loading was typically 10 mg per cell, composed of electroactive material mixed and grounded with Super P carbon in the weight ratio of 80:20. The separator was a porous polymer Celgard 2500 soaked with electrolyte, the latter consisting of 1 M lithium hexafluorophosphate in ethylene carbonate (EC)/diethyl carbonate (DEC) (1:1 w/w, LP30 commercial name). Finally, a lithium metal foil (Alfa Aesar) served both as reference and counter electrode. Galvanostatic measurements were performed using a Biologic VMP-3 potentiostat in the voltage window of 2.0–4 or 4.5V at different C-rates.

### 2.3 Synthesis and washing procedures

#### *Synthesis of nanometric $LiFePO_4$ (LFP NP)*

LFP nanoparticles were synthesized by employing oleylamine as capping and reducing agent; as reported elsewhere.[27] In brief, 16.8 mmol of LiI, 12.5 mmol of $(NH_4)_2HPO_4$, 12.5 mmol of $FeCl_2$, 0.38 mmol of oleylamine, and 125 mL of 1-octadecene were stirred together in a 500 mL three-neck flask under vacuum. The solution was maintained under vacuum at 120 °C

for 2 h and then heated at 250 °C under argon for 2 h. After precipitation using chloroform, LFP nanoparticles were recovered by centrifugation at 10000 rpm, followed by ethanol washing and vacuum drying.

*Washing with an organic solvent*

100 mg of LFP nanoparticles were dispersed in a mixture of chloroform and methanol 1:3 v/v (both Sigma-Aldrich) and vigorously stirred for one hour before being centrifugated. This process was repeated several times and followed by vaccum drying.

*Acid treatment using hydrochloric or acetic acid*

100 mg of LFP nanoparticles dispersed in 10 ml of ethanol were stirred with an acidic aqueous solution of hydrochloric acid with a concentration between 0.01 M - 0.5 M, or acetic acid with a concentration of 0.1 or 0.01 M. After 18h of stirring, the nanoparticles were collected by centrifugation at 8000 rpm, washed with ethanol and vacuum dried overnight.

*Ligand exchange - grafting*

20 mg of an organic molecule (2-carboxy-anthraquinone or 4-carboxy-TEMPO) were dissolved in dichloromethane and 100 mg of LFP nanoparticles were then added to the flask. The mixture was stirred during 6, 12, 24, 65 and 120 h in order to allow the complete exchange of the OlAm (24 h was chosen as the best). The hybrid material was collected by centrifugation at 8000 rpm and washed to remove ungrafted redox molecules.

## 3. Results and discussions

### *3.1 Characterization of OlAm-LFP*

Before any modification, as-synthesized LFP nanoparticles were analyzed to ensure their purity and electrochemical activity. The average size of the LFP nanoparticles was found to be 150 nm x 25 nm and aggregated in bundles of four nanorods (Figure 2a). The SAED pattern exhibits rings related to the nanometric crystals (figure 2b). The simulation pattern is consistent with the *Pnma* structure of $LiFePO_4$ (Figure 2c). Powder XRD analysis was carried

out to confirm the crystal structure (Figure 2d). The pattern can be assigned to triphylite, which crystal structure has been well studied for almost 20 years.[28] Indeed, the present result is consistent with previous refinements in an orthorhombic structure with the *Pnma* space group. In conventional solid-state reactions, high-temperature post-treatments are needed to prepare crystalline LFP nanoparticles. Through the procedure presented in this work, a rather simple solvothermal and inexpensive method allowed the synthesis of crystalline LFP nanoparticles at a maximum temperature of 260 ºC. During the synthesis, oleylamine was used both as a capping and reducing agent. The chemisorption affinity to surfacic metals is due to the Lewis interaction through the lone electron pair of the $NH_2$ functional group. Oleylamine coverage was evidenced by FTIR spectroscopy in the diffuse reflectance mode, an ideal technique to collect information from the surface even at small concentrations of organic species (Figure 2e). The infrared spectrum of LFP comprises the fundamental bending ($\delta$) and stretching ($\nu$) vibrations of the $PO_4^{3-}$ polyanions in the olivine structure observed at 660 $cm^{-1}$, 980$cm^{-1}$, 1170$cm^{-1}$, 1240 $cm^{-1}$ and 1630 $cm^{-1}$.[29] Besides, the presence of oleylamine is underlined by the vibration bands at 2922 $cm^{-1}$, 2854 $cm^{-1}$, 1410 $cm^{-1}$ and 1260 $cm^{-1}$ corresponding to $\upsilon_{as}$(C-H), $\upsilon_s$(C-H), $\delta(CH_3)$ and $\delta$ (N-H) respectively.[30,31] As expected, the electrochemical performance of OlAm-LFP, with only a capacity of 28 $mAh.g^{-1}$ (Figure 2f), is poor compared to carbon-coated LFP.[27] This low capacity can originate from the intrinsically poor electrical conductivity of LFP, and also to the presence of oleylamine on the surface thus electrically insulating LFP particles.

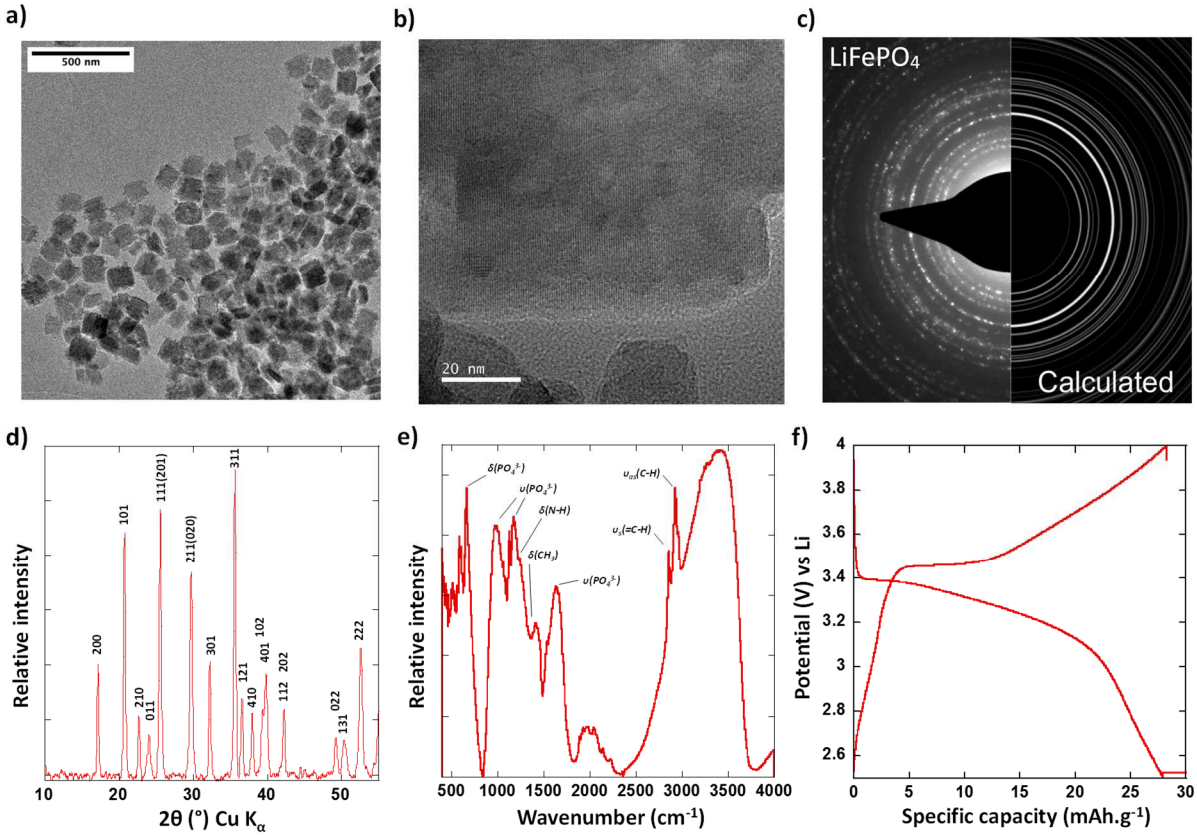


**Figure 2: Characterization of as-prepared OlAm-LFP using bright field TEM and HRTEM images (a and b), Selected-Area Electron Diffraction pattern (c), powder XRD (d) and FTIR in diffuse reflectance mode (e). Potential-composition profile of the OlAm-LFP nanoparticles mixed with 20% of carbon Super P and galvanostatically cycled between 2.5-4V at C/20 rate and using LP30 as electrolyte (f).**

At this stage, a carbon coating approach could have been the next logical step to overcome the electrical limitations and to provide better electrochemical performances. However, for the sake of understanding and to find a softer alternative, we focused here on the impact of different chemical surface modifications on these performances.

*3.2 Oleylamine removal using an organic solvent mixture*

The presence of oleylamine on the surface hampers the contact with carbon additive and inter LFP particles contact, and thus the charge transfer at the interface. Thus, a classical washing procedure with a solvent mixture, generally used to recover metal and metal oxide nanoparticles, was firstly carried out.[31] For that, chloroform and methanol were associated owing to the solubility of oleylamine in this solvent mixture and previous success of this

methodology for other nanomaterials. The nanoparticles were placed in the solvent mixture for one hour under stirring before being recovered by centrifugation. This operation, which has no effect on the LFP phase as seen on the XRD pattern (Figure 3b), was repeated until no evolution of the oleylamine related bands was anymore observed by FTIR (Figure 3a). After five washing cycles, the signals of oleylamine at 2922 $cm^{-1}$ and 2854 $cm^{-1}$ decrease drastically leading to particles almost free of capping agent. Unfortunately, even if most of oleylamine molecules was removed, the electrochemical activity was found to be very close to the activity obtained for an as-synthesized OlAm-LFP with 28 $mAh.g^{-1}$ (Figure 3c) confirming that the materials properties are more likely limited by the electrical conductivity limitation of LFP than by charge transfer at the interface.

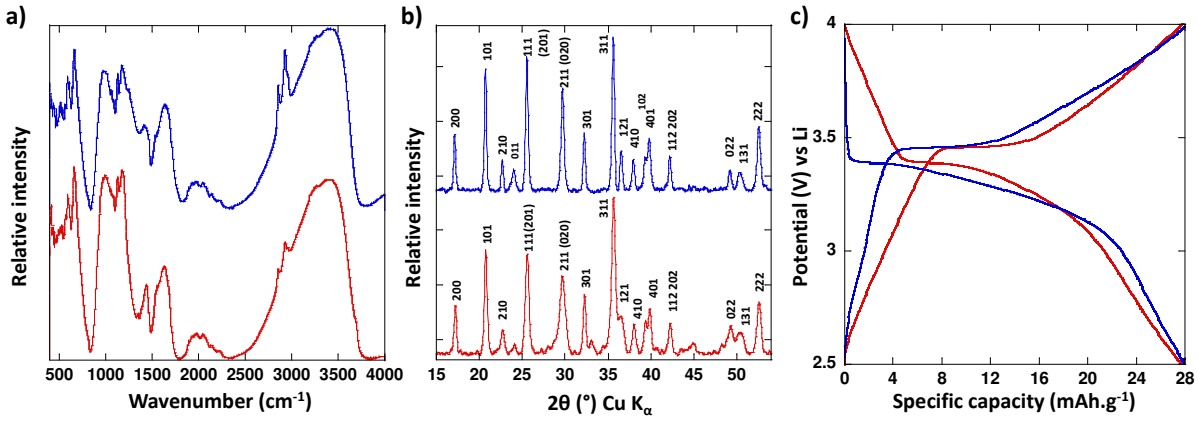


**Figure 3: Comparison between LFP nanoparticles before (blue curve) and after five washing with chloroform/methanol mixture (red curve) by FTIR (a), powder X-ray diffraction (b) and galvanostatic cycling (c). Electrochemical tests were realized using composite made of 80% of active material mixed with 20% of carbon Super P and galvanostatically cycled between at C/20 rate and using LP30 as the electrolyte.**

*3.3 Oleylamine removal using weak acid treatment*

Washing OlAm-LFP with an aqueous solution of $LiPF_6$ (such a solution is instable and leads to the *in-situ* generation of HF) was previously reported to be very beneficial as prior treatment to the carbon coating step.[27] This step is importance since it allows not only to clean the surface by removing oleylamine, but also to increase the specific surface area by

creating surface roughness, which makes the carbon coating more adhesive. On the basis of that study, the acidic treatment seems to be a good alternative since the protonation of the amine will provoke the departure of the capping agent through the quaternization of the free amine and generation of a positively charged entity (strong electrostatic repulsion with the surface). However, it is well-known that LFP can dissolve in acidic media, so this step should be managed very carefully. To prevent this latter, we investigated the washing of the OlAm-LFP nanoparticles with acetic acid, a weaker acid, with a higher pKa than HF (4.5 against 3.1 for HF), to successfully perform oleylamine removal.[32] Different concentrations of acetic acid (pure acetic acid, 0.1M and 0.01 M in bi-distilled water) were tested to optimize the removal of the capping agent whilst limiting either surface attack or delithiation of the material (surface formation of $FePO_4$). Note that in the case of pure acetic acid, the material partially dissolved, and the obtained solid turns to a grey/blueish colour indicating that a chemical reaction took place. Interestingly, by increasing the concentration, signals related to oleylamine at 2922 $cm^{-1}$, 2854 $cm^{-1}$, 1410 $cm^{-1}$ and 1260 $cm^{-1}$ progressively disappear which implies that the capping-agent is removed efficiently (Figure 4a). Nevertheless, in all the cases it is important to note the strong modifications of the signals from LFP at 660 $cm^{-1}$, 980$cm^{-1}$, 1170$cm^{-1}$, 1240 $cm^{-1}$; this latter completely vanished, which suggests the probable transformation of the inorganic surface (FTIR in a diffuse reflectance mode shows only material surface).[29] XRD analysis carried out on these samples confirms chemical delithiation and formation of $FePO_4$, observed at 17.9°, 22.8°, 30.1/30.7° (Figure 4b).[33] When using 0.1 M or 0.01 M acetic acid solutions, these peaks appear less intense meaning that chemical delithiation took place on the surface of the nanoparticles to form core-shell particles (Core-Shell-LFP) as confirmed by HRTEM imaging (Figure 4d). After these treatments, the electrochemical activity was improved following the rise of acetic acid concentration which increased with respectively 52 $mAh.g^{-1}$ and 72 $mAh.g^{-1}$, for 0.01M and

0.1M concentrations, but remains far from the theoretical capacity (Figure 4c). In the case of pure acetic acid, the capacity was still low at 63 $mAh.g^{-1}$ and a change in the shape of the oxidation curve is observed.

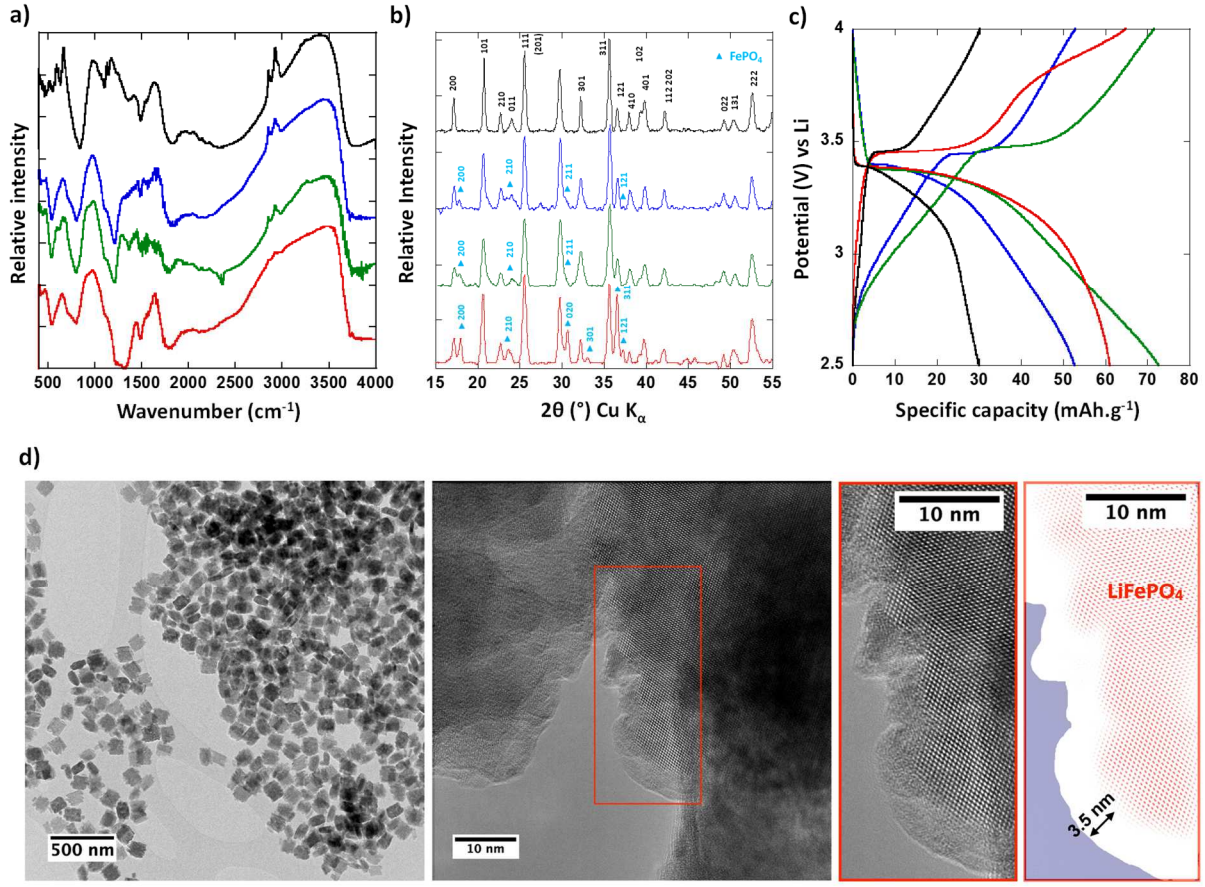


**Figure 4: Comparison between LFP nanoparticles before (black curve) and after washing with pure acetic acid (red curve), 0.1 M acetic acid solution (green curve) and 0.01 acetic acid solution (blue curves) by FTIR in diffuse reflectance mode (a) and powder X-ray diffraction (b). Electrochemical tests performed with LFP nanoparticles before (black curve) and after washing with pure (red curve), 0.1 M (green curve) and 0.01 (blue curve) acetic acid solutions. Active materials were mixed with 20% of carbon Super P and galvanostatically cycled at C/20 rate and using LP30 as electrolyte. High-Resolution Transmission Electronic Microscopy micrographs of OlAm-LFP nanoparticles washed with a 1M aqueous acetic acid solution (d).**

*3.4 Grafting of redox molecule through a ligand exchange reaction*

Another possible alternative to avoid the time and energy-consuming formation of carbon coating is to take benefit of organic-based compounds chemically grafted on the particles.

Indeed, in the past, dyes like BMABP (4-[bis(4-methoxyphenyl)amino]benzylphosphonic acid) or Z907Na (amphiphilic heteroleptic ruthenium complex) and conducting polymers, such as PANI, PPy, PEDOT, were successfully employed to solve conductivity issues.[20,22,34–37] Through another approach, non-conjugated redox-active polymers based on TEMPO and thianthrene moieties have been associated with positive electrode materials to boost charge/discharge kinetics using redox potential overlapping.[23,26,38] With this in mind, this work intends to bring a new dimension by focusing on single molecules directly grafted on the surface of the electroactive material. Exploration of surface grafting by chemical anchoring is of interest since controlling the surface organization could first maximize surface conductivity by electron hopping and/or ionic diffusion[39] and secondly afford an additional capacity. Two well-known redox probes were used as references for our study: 4-Carboxy-TEMPO displaying a redox activity at 3.5V *vs* $Li/Li^+$ that fits the LFP redox potential, and another one well below, 2-carboxy-anthraquinone with redox activity situated at 2.4V *vs.* $Li/Li^+$. Carboxylic acid function was preferred for grafting since it has a natural affinity with metal cations[40,41] facilitating charge transfer reactions, compared with phosphonic acid.[42] Ligand exchange was carried out in dichloromethane to facilitate the removal of oleylamine, and the excess of solvent and redox molecule (Figure 5).

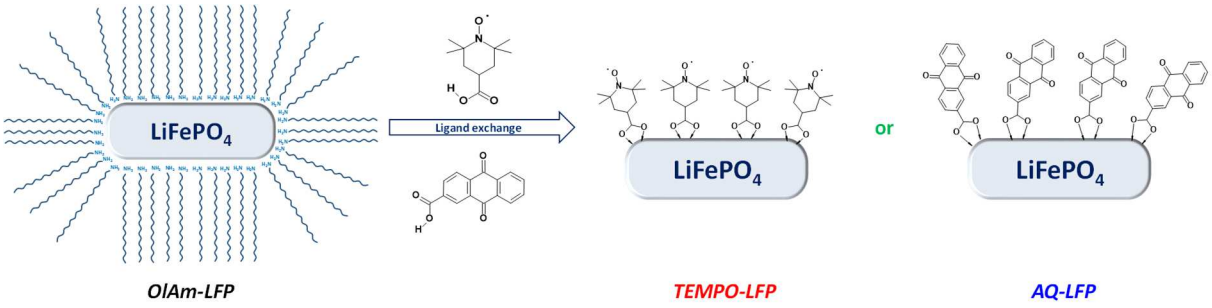


**Figure 5: Scheme illustrating oleylamine removal by surface anchoring of redox-active organic molecules possessing the carboxylic acid function.**

In both cases, ligand exchange was successful since oleylamine signals were removed from the FTIR spectra, concomitantly with the appearance of characteristic peaks of the grafted

redox molecules (Figure 6a and b). For TEMPO-based hybrid LFP (TEMPO-LFP), signals attributed to the methylene group of the nitroxide derivative are observed at 2993 $cm^{-1}$, 2929 $cm^{-1}$ and 2854 $cm^{-1}$. Other characteristics peaks are also distinctly depicted at 930 $cm^{-1}$, 1133 $cm^{-1}$, 1175 $cm^{-1}$, 1250 $cm^{-1}$, 1345 $cm^{-1}$, 1412 $cm^{-1}$ and 1458 $cm^{-1}$, the good preservation of this derivative upon grafting is evidenced with only a small frequency shift in the spectra. Another important information underlined by FT-IR is the proof of chemical grafting through the absence of band corresponding to residual ungrafted carboxylic acid (normally observed at 1691 $cm^{-1}$) and the presence of the carboxylate band observed at 1533 $cm^{-1}$. The latter indicates that the redox molecule is strongly associated with the surface through a coordinative anchoring and presumably *via* a bidentate mode.[43] Similar conclusions can be made for the anthraquinone-based hybrid LFP (AQ-LFP) , which displays characteristic peaks of the anthraquinone core at 1286 $cm^{-1}$, 1325 $cm^{-1}$, 1403 $cm^{-1}$, 1481 $cm^{-1}$, 1597 $cm^{-1}$, 1679 $cm^{-1}$ and appearance of the carboxylate band at 1551 $cm^{-1}$ (initially present at 1710 $cm^{-1}$ in its acid form). Note that no modifications on the XRD pattern are observed, indicating that $FePO_4$ was not formed during grafting, in constrat with the acetic acid treatment (Figure 6c).

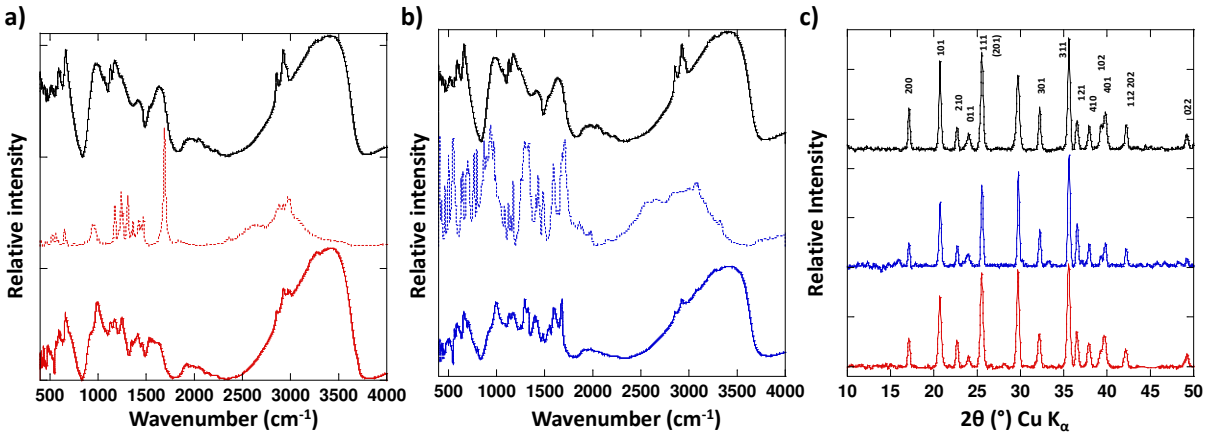


**Figure 6: Comparison between OlAm-LFP nanoparticles before (black curve) and after ligand exchange reaction with 4-carboxy-TEMPO (red curve) and 2-carboxy-anthraquinone (blue curve) by FT-IR in diffuse reflectance mode (a and b) and powder XRD patterns (c). The corresponding starting redox molecules are displayed in doted lines on FT-IR spectra.**

The electrochemical activity of organically modified LFP was then studied under the same conditions as OlAm-LFP and using the same formulation and battery conditions. It is interesting to note that different behaviours are evidenced for the two hybrids materials. When modified with anthraquinone, no major effect was observed on the electrochemical curve, except for a very small improvement of the capacity (+15 $mA.g^{-1}$), coming from the grafted anthraquinone clearly identified around 2.4V *vs.* $Li/Li^+$ (Figure 7a and b). On the contrary, with TEMPO the electrochemical activity changes drastically (Figure 7c). First, the capacity of the hybrid increases drastically reaching more than 100 $mAh.g^{-1}$ in the first cycle. More importantly, the curve shape becomes very flat with a smooth plateau, associated with low polarization. This is very intriguing since solid solution curve type are generally obtained with very small particle size, notably for LFP.[44] In the present case, a pure biphasic behaviour is obtained. This fact could be explained by the very high reaction kinetic of TEMPO and fast charge transfer between organic molecule and material when molecule is grafted compared with simple blending of LFP with PTMA polymer.

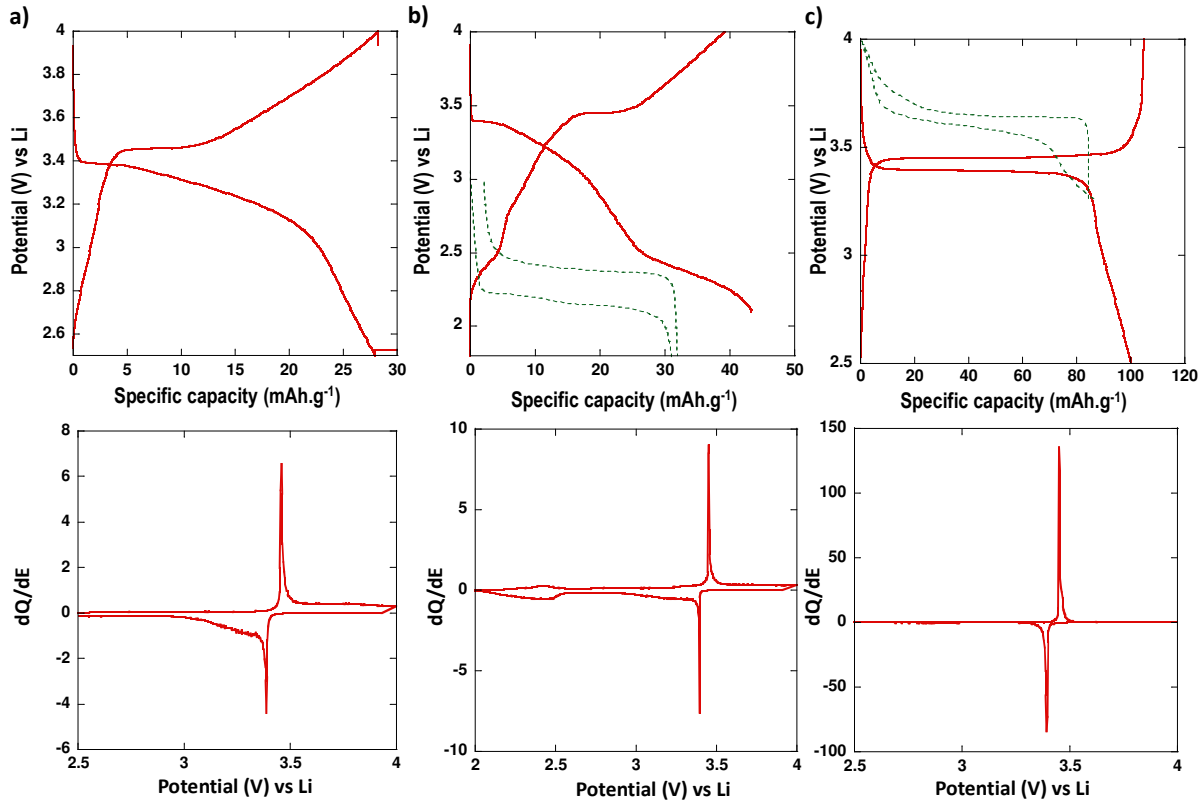

**Figure 7: Potential-composition profiles and their corresponding derivatives of OlAm-LFP (a), AQ-LFP (b) and TEMPO-LFP (c). The electrochemical activity of single molecules is also displayed as dotted line (b and c). Active materials were mixed with 20% of carbon Super P and galvanostatically cycled at a C/20 rate and using LP30 as the electrolyte.**

In this case, the electrochemical signal coming from the TEMPO-based molecule, initially observed at around 3.6V *vs.* $Li/Li^+$ when tested as free molecule (doted line figure 7b), is completely absent as if the redox molecule became inactive when grafted. Note also that the polarisation is quite small. Most probably, the redox potential of TEMPO is affected by the grafting process and is strongly associated with the LFP to give a new conjugated particle in which the TEMPO acts as an electron mediator for charging/discharging LFP nanoparticles. This phenomenon is explained by the overlapping of the redox potential coupled with the spatial proximity between the redox probe and LFP surface, which favour fast electron transfer (Figure 8). During oxidation, the nitroxide radical is fastly oxidized to an oxoammonium reacting quickly with $LiFePO_4$ to give $FePO_4$ and forming back the nitroxide radical. The inverse mediated reaction seems to be more difficult to achieve since coulombic efficiency is not equal to 100%, traduced as limited charge transfer during reduction, perhaps due to a slight mismatch of the electrochemical potential of the two redox systems.

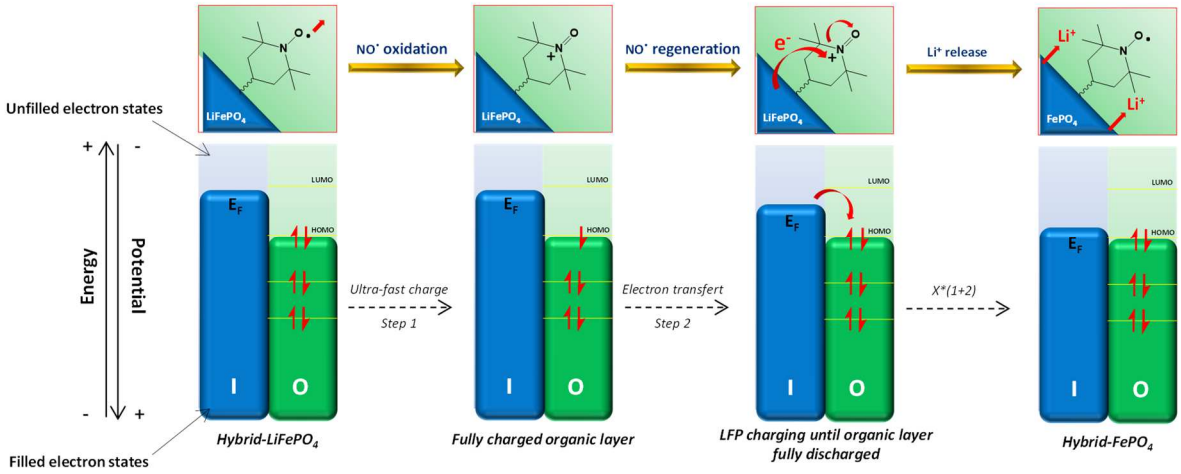


**Figure 8: Representation of the charge transfer mechanism during oxidation in the hybrid TEMPO-LFP positive electrode.**

Following this interesting result, the activity of TEMPO-LFP at different current densities was investigated. For the sake of clarity, they are compared with free-LFP obtained by washing with an acetic acid solution (0.1M). At a C/30 rate, TEMPO-LFP displays a flat signal at 3.42V *vs* $Li^+/Li$ associated with a specific capacity of 108 $mAh.g^{-1}$, while free-LFP shows large polarization (more than 500 mV) and a lower specific capacity of 81 $mAh.g^{-1}$ (Figure 9a). When increasing the rate to C-rate and 5C-rate, the difference between the different compounds become more pronounced. At these speeds, TEMPO-LFP still shows a relatively high capacity during the first oxidation with respectively 101 $mAh.g^{-1}$ and 92 $mAh.g^{-1}$, whilst Free-LFP displays only 13 $mAh.g^{-1}$ and no capacity (Figure 9b and c). Going from C/30 to C-rate induces an increase of the polarization especially for the reduction process, showing the mediation process is strongly affected and appears to be less effective. This phenomenom can be explained by the disrupting of the charge transfer between organic probe and LFP surface for the reduction (overlapping less efficient to allow charge transfer during the reduction).

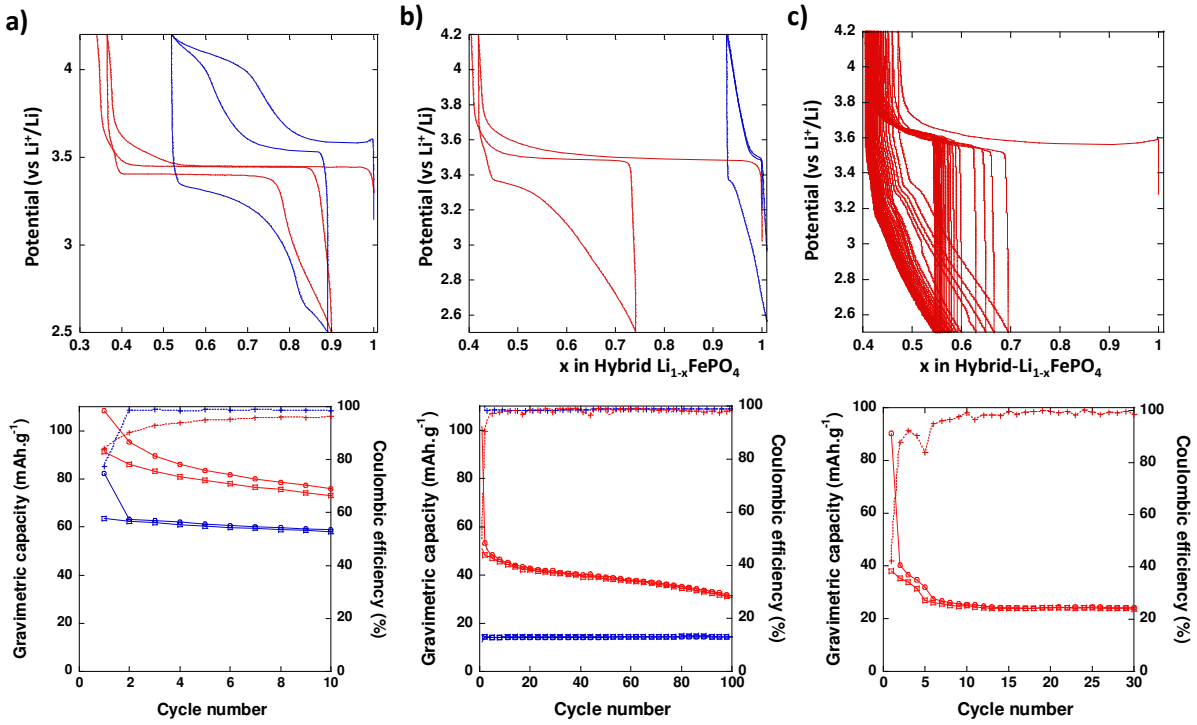


**Figure 9: Potential-composition profiles, associated capacity retention and coulombic efficiency of Free-LFP (blue curve) and hybrid TEMPO-LFP (red curve) mixed with 20% of Csp and**

**galvanostatically cycled between 2.5-4V *vs.* Li/Li$^+$ and using LP30 as electrolyte at C/30 rate (a), C-rate (b) and 5C-rate (c).**

Even if the redox reactivity of the TEMPO is not perfectly aligned with the reduction potential of LFP, it is interesting to note that such charge transfer concept, carried out directly over the surface, allow to apply a continuous C-rate, compared with simple blending with a nitroxide-based polymer. This, let us think that accordingly to a accurate surface organisation or oligomer grafting, better performances could be improved, paving the way toward more efficient materials without a carbon coating step and with improved storage performances. In the future, it would be interesting to extend this approach to more oxidative materials like NMC or LMO by tuning the redox potential of the redox probe, either by molecular design or used of other mediators like phenothiazine or thianthrene[45–47] or by electrolyte engineering using specific additives or solvents,[48] to make charge transfer as efficient as possible.

## 4. Conclusions

This study highlights, for the first time, the impact of grafting redox mediators and its redox potential on the electrochemical properties of an inorganic material currently used in the field of energy storage. A specific focus was made on the surface modification of LFP nanoparticles obtained by a solvothermal method in the presence of oleylamine used as both reducing and capping agent to limit particle size growth. Different methods were used to remove the capping agent and allowed to underline the limitations of the LFP active material without carbon coating, as previously reported. On the other hand, the exchange of the capping agent and chemical grafting of a TEMPO derivative, exhibiting redox potential overlapping the redox potential of LFP, has proven to be very interesting since it allows to generate a charge transfer mechanism leading to the a drastic change of the electrochemical signal and an improvement of the electrochemical performances. Even if the performances remain behind the use of a carbon coating, it opens the way to a softer alternative which will facilitate the formulation of electrodes by removing the energy-consuming heat treatment step

and could facilitate the recycling of the active material at the end of the battery assembly. In the future, besides the exemplification of this approach with other electrode materials (NMC or LMO) associated with phenothiazine or thianthrene derivatives, a deep understanding of the molecule surface organization to favor electronic percolation phenomenom is mandatory to clearly address the question of the definitive replacement of carbon-coating.

**ACKNOWLEDGEMENTS**

A.C.M. was supported by the EMJMD program of the European Union, through a scholarship for the ERASMUS MUNDUS Master Program "Materials for Energy Storage and Conversion (M.E.S.C.). The region Hauts-de-France (HdF) and the French Research Network on Electrochemical Energy Storage (RS2E) are gratefully acknowledged for financial support through grants accorded respectively to M.R. and W. D.

**CONFLICT OF INTEREST**

The authors declare no conflict of interest.

**REFERENCES**

[1] B. Dunn, H. Kamath, J.-M. Tarascon, Electrical Energy Storage for the Grid: A Battery of Choices, Science (80-. ). 334 (2011) 928–935. https://doi.org/10.1126/science.1212741.

[2] C. Masquelier, L. Croguennec, Polyanionic (phosphates, silicates, sulfates) frameworks as electrode materials for rechargeable Li (or Na) batteries, Chem. Rev. 113 (2013) 6552–6591. https://doi.org/10.1021/cr3001862.

[3] N. Nitta, F. Wu, J.T. Lee, G. Yushin, Li-ion battery materials: present and future, Mater. Today. 18 (2015) 252–264. https://doi.org/10.1016/j.mattod.2014.10.040.

[4] P. Poizot, S. Laruelle, S. Grugeon, L. Dupont, J.-M. Tarascon, Nano-sized transition-

metal oxides as negative-electrode materials for lithium-ion batteries, Nature. 407 (2000) 496–499. https://doi.org/10.1038/35035045.

[5] J. Lu, Z. Chen, Z. Ma, F. Pan, L.A. Curtiss, K. Amine, The role of nanotechnology in the development of battery materials for electric vehicles, Nat. Nanotechnol. 11 (2016) 1031–1038. https://doi.org/10.1038/nnano.2016.207.

[6] H.K. Liu, G.X. Wang, Z. Guo, J. Wang, K. Konstantinov, Nanomaterials for Lithium-ion Rechargeable Batteries, J. Nanosci. Nanotechnol. 6 (2006) 1–15. https://doi.org/10.1166/jnn.2006.103.

[7] Y. Sun, N. Liu, Y. Cui, Promises and challenges of nanomaterials for lithium-based rechargeable batteries, Nat. Energy. 1 (2016) 16071. https://doi.org/10.1038/nenergy.2016.71.

[8] H. Li, H. Zhou, Enhancing the performances of Li-ion batteries by carbon-coating: present and future, Chem. Commun. 48 (2012) 1201–1217. https://doi.org/10.1039/C1CC14764A.

[9] R. Dominko, M. Bele, M. Gaberscek, M. Remskar, D. Hanzel, S. Pejovnik, J. Jamnik, Impact of the Carbon Coating Thickness on the Electrochemical Performance of LiFePO[sub 4]/C Composites, J. Electrochem. Soc. 152 (2005) A607. https://doi.org/10.1149/1.1860492.

[10] J. Wang, X. Sun, Understanding and recent development of carbon coating on LiFePO 4 cathode materials for lithium-ion batteries, Energy Environ. Sci. 5 (2012) 5163–5185. https://doi.org/10.1039/c1ee01263k.

[11] N. Recham, J.N. Chotard, L. Dupont, C. Delacourt, W. Walker, M. Armand, J.M. Tarascon, A 3.6 v lithium-based fluorosulphate insertion positive electrode for lithium-ion batteries, Nat. Mater. 9 (2010) 68–74. https://doi.org/10.1038/nmat2590.

[12] P. Judeinstein, C. Sanchez, Hybrid organic-inorganic materials : a land of

multidisciplinarity Chemistry : Synthesis of Hybrid Materials, J. Mat. Chem. 6 (1996) 511–525. https://doi.org/https://doi.org/10.1039/JM9960600511.

[13] C. Sanchez, B. Julián, P. Belleville, M. Popall, Applications of hybrid organic-inorganic nanocomposites, J. Mater. Chem. 15 (2005) 3559–3592. https://doi.org/10.1039/b509097k.

[14] O. Brian, G. Michael, A low-cost, high-efficiency solar cell based on dye-sensitized colloidal TiO2 films, Nature. 353 (1991) 737–740. https://doi.org/10.1016/0146-5724(84)90144-4.

[15] M. Grätzel, Dye-sensitized solar cells, J. Photochem. Photobiol. C Photochem. Rev. 4 (2003) 145–153. https://doi.org/10.1016/S1389-5567(03)00026-1.

[16] M. Lira-cantu, P. Gomez-Romero, The Organic-Inorganic Polyaniline / V 2 O 5 System Application as a High-Capacity Hybrid Cathode for Rechargeable Lithium Batteries, J. Electrochem. Soc. 146 (1999) 2029–2033.

[17] P. Gomez-Romero, Hybrid organic-inorganic materials - in search of synergic activity, Adv. Mater. 13 (2001) 163–174. https://doi.org/10.1002/1521-4095.

[18] K. Jurewicz, S. Delpeux, V. Bertagna, F. Béguin, E. Frackowiak, Supercapacitors from nanotubes/polypyrrole composites, Chem. Phys. Lett. 347 (2001) 36–40. https://doi.org/10.1016/S0009-2614(01)01037-5.

[19] D. Bélanger, X. Ren, J. Davey, F. Uribe, S. Gottesfeld, Characterization and Long-Term Performance of Polyaniline-Based Electrochemical Capacitors, J. Electrochem. Soc. 147 (2000) 2923. https://doi.org/10.1149/1.1393626.

[20] L. Kavan, I. Exnar, J. Cech, M. Graetzel, Enhancement of electrochemical activity of LiFePO4 (olivine) by amphiphilic ru-bipyridine complex anchored to a carbon nanotube, Chem. Mater. 19 (2007) 4716–4721. https://doi.org/10.1021/cm071107p.

[21] Q. Wang, S.M. Zakeeruddin, D. Wang, I. Exnar, M. Grätzel, Redox targeting of

insulating electrode materials: A new approach to high-energy-density batteries, Angew. Chemie - Int. Ed. 45 (2006) 8197–8200. https://doi.org/10.1002/anie.200602891.

[22] A. Sobkowiak, M.R. Roberts, R. Younesi, T. Ericsson, L. Häggström, C.W. Tai, A.M. Andersson, K. Edström, T. Gustafsson, F. Björefors, Understanding and controlling the surface chemistry of LiFeSO4F for an enhanced cathode functionality, Chem. Mater. 25 (2013) 3020–3029. https://doi.org/10.1021/cm401063s.

[23] A. Vlad, N. Singh, J. Rolland, S. Melinte, P.M. Ajayan, Hybrid supercapacitor-battery materials for fast electrochemical charge storage, Sci. Rep. 4 (2014) 1–7. https://doi.org/10.1038/srep04315.

[24] Q. Huang, L. Cosimbescu, P. Koech, D. Choi, J.P. Lemmon, Composite organic radical e inorganic hybrid cathode for lithium-ion batteries, J. Power Sources. 233 (2013) 69–73. https://doi.org/10.1016/j.jpowsour.2013.01.076.

[25] G. Dolphijn, S. Isikli, F. Gauthy, A. Vlad, J.F. Gohy, Hybrid LiMn2O4–radical polymer cathodes for pulse power delivery applications, Electrochim. Acta. 255 (2017) 442–448. https://doi.org/10.1016/j.electacta.2017.10.021.

[26] K. Hatakeyama-Sato, T. Masui, T. Serikawa, Y. Sasaki, W. Choi, S.G. Doo, H. Nishide, K. Oyaizu, Nonconjugated Redox-Active Polymer Mediators for Rapid Electrocatalytic Charging of Lithium Metal Oxides, ACS Appl. Energy Mater. 2 (2019) 6375–6382. https://doi.org/10.1021/acsaem.9b01007.

[27] A. Paolella, G. Bertoni, S. Marras, E. Dilena, M. Colombo, M. Prato, A. Riedinger, M. Povia, A. Ansaldo, K. Zaghib, L. Manna, C. George, Etched colloidal LiFePO4 nanoplatelets toward high-rate capable Li-ion battery electrodes, Nano Lett. 14 (2014) 6828–6835. https://doi.org/10.1021/nl504093w.

[28] G. Rousse, J. Rodriguez-Carvajal, S. Patoux, C. Masquelier, Magnetic Structures of the

Triphylite LiFePO4 and of Its Delithiated Form FePO4, Chem. Mater. 15 (2003) 4082–4090. https://doi.org/10.1021/cm0300462.

[29] A.A. Salah, P. Jozwiak, J. Garbarczyk, F. Gendron, A. Mauger, C.M. Julien, FTIR features of lithium iron phosphates used as positive electrodes in rechargeable lithium batteries, Proc. - Electrochem. Soc. PV 2005-14 (2008) 103–112.

[30] S. Mourdikoudis, L.M. Liz-Marzán, Oleylamine in nanoparticle synthesis, Chem. Mater. 25 (2013) 1465–1476. https://doi.org/10.1021/cm4000476.

[31] Z. Xu, C. Shen, Y. Hou, H. Gao, S. Sun, Oleylamine as both reducing agent and stabilizer in a facile synthesis of magnetite nanoparticles, Chem. Mater. 21 (2009) 1778–1780. https://doi.org/10.1021/cm802978z.

[32] D. Li, C. Wang, D. Tripkovic, S. Sun, N.M. Markovic, V.R. Stamenkovic, Surfactant removal for colloidal nanoparticles from solution synthesis: The effect on catalytic performance, ACS Catal. 2 (2012) 1358–1362. https://doi.org/10.1021/cs300219j.

[33] M.H. Lee, T.H. Kim, Y.S. Kim, J.S. Park, H.K. Song, Optimized evolution of a secondary structure of LiFePO4: Balancing between shape and impurities, J. Mater. Chem. 22 (2012) 8228–8234. https://doi.org/10.1039/c2jm30403a.

[34] D. Lepage, C. Michot, G. Liang, M. Gauthier, S.B. Schougaard, A soft chemistry approach to coating of LiFePO4 with a conducting polymer, Angew. Chemie - Int. Ed. 50 (2011) 6884–6887. https://doi.org/10.1002/anie.201101661.

[35] Y. Huang, J.B. Goodenough, High-Rate LiFePO Lithium Rechargeable Battery Promoted by Electrochemically Active Polymers High-Rate LiFePO 4 Lithium Rechargeable Battery Promoted by Electrochemically Active Polymers, (2008) 7237–7241. https://doi.org/10.1021/cm8012304.

[36] Y.M. Bai, P. Qiu, Z.L. Wen, S.C. Han, Improvement of electrochemical performances of LiFePO4 cathode materials by coating of polythiophene, J. Alloys Compd. 508

(2010) 1–4. https://doi.org/10.1016/j.jallcom.2010.05.173.

[37] Q. Wang, N. Evans, S.M. Zakeeruddin, I. Exnar, M. Grätzel, Molecular Wiring of Insulators : Charging and Discharging Insulating Electrode Materials in High Energy Lithium-Ion Batteries by Molecular Charge Transport Layers, J. Am. Chem. Soc. 129 (2007) 3163–3167. https://doi.org/10.1021/ja066260j.

[38] G. Dolphijn, S. Isikli, F. Gauthy, A. Vlad, J.F. Gohy, Hybrid LiMn2O4–radical polymer cathodes for pulse power delivery applications, Electrochim. Acta. 255 (2017) 442–448. https://doi.org/10.1016/j.electacta.2017.10.021.

[39] J. Bidal, M. Becuwe, C. Hadad, B. Fleutot, C. Davoisne, M. Deschamps, B. Porcheron, A.N. Van Nhien, Hybrid Electrolytes Based on Optimized Ionic Liquid Quantity Tethered on ZrO2 Nanoparticles for Solid-State Lithium-Ion Conduction, ACS Appl. Mater. Interfaces. 13 (2021) 15159–15167. https://doi.org/10.1021/acsami.0c22422.

[40] M. Neouze, U. Schubert, Surface Modification and Functionalization of Metal and Metal Oxide Nanoparticles by Organic Ligands, Monatshefte Fur Chemie. 139 (2008) 183–195. https://doi.org/10.1007/s00706-007-0775-2.

[41] M. Omri, M. Becuwe, M. Courty, G. Pourceau, A. Wadouachi, Nitroxide-Grafted Nanometric Metal Oxides for the Catalytic Oxidation of Sugar, ACS Appl. Nano Mater. 2 (2019) 5200–5205. https://doi.org/10.1021/acsanm.9b01069.

[42] A. Baktash, B. Khoshnevisan, A. Sasani, K. Mirabbaszadeh, Effects of carboxylic acid and phosphonic acid anchoring groups on the efficiency of dye sensitized solar cells: A computational study, Org. Electron. 33 (2016) 207–212. https://doi.org/10.1016/j.orgel.2016.03.013.

[43] M. Omri, M. Becuwe, G. Pourceau, C. Davoisne, A. Wadouachi, Nitroxide supported on nanometric metal oxides as new hybrid catalysts for selective sugar oxidation, J. Colloid. Interf. Sci. 536 (2019) 526–535. https://doi.org/10.1016/j.jcis.2018.10.065.

[44] C. Delacourt, P. Poizot, S. Levasseur, C. Masquelier, Size Effects on Carbon-Free LiFePO 4 Powders The Key to Superior Energy Density, Electrochem. Solid State Lett. 9 (2006) 352–355. https://doi.org/10.1149/1.2201987.

[45] A.E. Lakraychi, F. Dolhem, F. Djedaïni-Pilard, M. Becuwe, Substituent effect on redox potential of terephthalate-based electrode materials for lithium batteries, Electrochem. Commun. 93 (2018) 71–75. https://doi.org/10.1016/j.elecom.2018.06.009.

[46] A.E. Lakraychi, E. Deunf, K. Fahsi, P. Jimenez, J.-P. Bonnet, F. Djedaini-Pilard, M. Bécuwe, P. Poizot, F. Dolhem, An air-stable lithiated cathode material based on a 1,4-benzenedisulfonate backbone for organic Li-ion batteries, J. Mater. Chem. A. 6 (2018) 19182–19189. https://doi.org/10.1039/C8TA07097K.

[47] L. Sieuw, A.E. Lakraychi, D. Rambabu, K. Robeyns, A. Jouhara, G. Borodi, C. Morari, P. Poizot, A. Vlad, Through-Space Charge Modulation Overriding Substituent Effect: Rise of the Redox Potential at 3.35 v in a Lithium-Phenolate Stereoelectronic Isomer, Chem. Mater. 32 (2020) 9996–10006. https://doi.org/10.1021/acs.chemmater.0c02989.

[48] H. Wang, R. Emanuelsson, A. Banerjee, R. Ahuja, M. Strømme, M. Sjödin, Effect of Cycling Ion and Solvent on the Redox Chemistry of Substituted Quinones and Solvent-Induced Breakdown of the Correlation between Redox Potential and Electron-Withdrawing Power of Substituents, J. Phys. Chem. C. 124 (2020) 13609–13617. https://doi.org/10.1021/acs.jpcc.0c03632.